Blind and Training-Assisted Subspace Code-Timing Estimation for CDMA With Bandlimited Chip Waveforms

Khaled Amleh, *Member, IEEE*, Hongbin Li, *Member, IEEE*, and Tao Li

***Abstract*—In this paper, we present a group of subspace code-timing estimation algorithms for asynchronous code-division multiple-access (CDMA) systems with bandlimited chip waveforms. The proposed schemes are frequency-domain based techniques that exploit a unique structure of the received signal in the frequency domain. They can be implemented either blindly or in a training-assisted manner. The proposed blind code-timing estimators require only the spreading code of the desired user, whereas the training-assisted schemes assume the additional knowledge of the transmitted symbols of the desired user. Through a design parameter of user choice, the proposed schemes offer flexible tradeoffs between performance, user capacity, and complexity. They can deal with both time- and frequency-selective fading channels. Numerical simulations show that the proposed schemes are near-far resistant, and compare favorably to an earlier subspace code-timing estimation scheme that is implemented in the time domain.**

***Index Terms*—Code-division multiple-access (CDMA), code-timing estimation and synchronization, bandlimited chip waveforms, time- and frequency-selective fading channels.**

I. Introduction

CODE-DIVISION MULTIPLE-ACCESS (CDMA) is considered a major air interface scheme for wireless mobile communications [1]. In CDMA systems, all user transmissions overlap in time and frequency. They are distinguished from one another by utilizing a unique spreading code for each user. In order to successfully recover the information of each transmission, the local spreading code generator has to be synchronized to the code-timing of the desired transmission. This is considered one of the most challenging tasks performed at a CDMA receiver [2, ch. 5].

Multiuser code-timing estimation and synchronization, which parallels the well acknowledged research on multiuser detection (e.g., [3]) for CDMA systems, has been receiving increasing interest recently. Most existing code-timing estimation techniques can be classified as either *training-assisted* methods that require transmission of training symbols known to the receiver to assist code acquisition, or *blind* techniques that obviate training but rely on the structure of spreading codes for code acquisition. Notable training-assisted schemes include the classical correlator [2, ch. 5], which is optimum only in the single-user case but very sensitive to multiple-access interference (MAI), and the more recently introduced, multiuser based methods, such as the minimum mean squared error (mmse) [4], maximum likelihood (ML), and large-sample ML (LSML) [5], [6] code synchronization algorithms, among others. A short list of blind code synchronization algorithms include the well-known subspace scheme [7], [8] and several variants [9]–[11], and the minimum variance based methods [12]–[14]. Compared with the single-user based correlator, these multiuser based code synchronization schemes achieve significantly improved performance in near-far environments, and can support more user transmissions without enforcing stringent power control.

Most of the aforementioned code-timing estimation schemes implicitly assume *rectangular* chip waveforms which are not bandlimited and seldom used in practice. Real CDMA systems utilize *bandlimited* chip waveforms, such as the square-root raised-cosine pulse [15]. In contrast with the rich research works on code-timing estimation with rectangular chip waveforms, only limited studies are available that take into account bandlimited chip waveforms. One possible approach to dealing with the problem is to extend existing methods by enforcing bandlimited chip waveforms in their cost functions. For example, the subspace technique, originally proposed in [7] and [8] for rectangular chip waveforms, was extended in [16] to handle bandlimited pulses. The extension is conceptually simple; however, the implementation is not. In particular, subspace methods for rectangular pulses can be conveniently implemented by low-complexity polynomial rooting, whereas the counterparts for bandlimited pulses involve highly nonlinear cost functions that require iterative nonlinear searches over the parameter space, a process that is computationally expensive and suffer local convergence due to inaccurate initialization (see Section V).

Another notable code-timing estimation scheme addressing bandlimited chip waveforms was recently proposed in [17]. It exploits various shift-invariance in the frequency domain to isolate the subspace of interest, from which an ESPRIT (see [18]) like procedure is invoked to derive the code-timing estimates. Unlike the extended subspace estimator of [16], the shift-invariance based algorithm is noniterative, requiring no parameter initialization. It works quite well in time-invariant channels [17].

Manuscript received July 13, 2003; revised March 16, 2004, May 15, 2004, and June 30, 2004. This work was supported in part by the New Jersey Commission on Science and Technology and by the Army Research Office by Grant DAAD19-03-1-0184.

K. Amleh is with the Department of Engineering, Pennsylvania State University, Mont Alto, PA 17237 USA (e-mail: kaa13@psu.edu).

H. Li is with the Department of Electrical and Computer Engineering, Stevens Institute of Technology, Hoboken, NJ 07030 USA (e-mail: hli@stevens.edu).

T. Li is with the Computer Department, Sichuan University, Chengdu 610065, P.R. China (e-mail:litao@scu.edu.cn).

Digital Object Identifier 10.1109/TVT.2004.836963

When the channel is both time- and frequency-selective, however, the algorithm was found to degrade significantly.

In this paper, we also take a subspace approach and present new solutions to the code-timing estimation problem with the bandlimited pulse constraint. In contrast to the earlier time-domain subspace technique of [16] that requires multidimensional searches, our proposed schemes are frequency-domain based techniques that can be conveniently implemented via rooting of a single-variate polynomial. Unlike the shift-invariance based method [17], our schemes can deal with both time- and frequency-selective fading channels, meanwhile providing resistance to strong MAI. The proposed schemes include a group of blind and training-assisted code-timing estimation algorithms that rely on frequency-domain subspace decomposition. Only the desired user's spreading code is required for the blind schemes. The training-assisted schemes also assume transmission of a unique training sequence for the desired user. By utilizing a design parameter of user choice that controls the subspace dimension, all proposed schemes allow convenient tradeoffs between estimation accuracy, user capacity, and implementation complexity.

The rest of the paper is organized as follows. In Section II, we introduce the data model and formulate the problem of interest. In Section III, we discuss a unique structure of the received signal in the frequency domain. A group of blind and training-assisted subspace code-timing estimators exploiting this structure are presented in Section IV. Section V contains numerical examples illustrating the performance of the proposed as well as competing schemes. Finally, we draw conclusions in Section VI.

Notation: Vectors (matrices) are denoted by boldface lower (upper) case letters; all vectors are column vectors; superscripts $(\cdot)^T$, $(\cdot)^*$, and $(\cdot)^H$ denote the transpose, conjugate, and conjugate transpose, respectively; $\mathbf{I}_N$ denotes the $N \times N$ identity matrix; $\mathbf{0}$ denotes an all-zero matrix or vector; $\mathrm{diag}\{\mathbf{x}\}$ denotes a diagonal matrix with the elements of $\mathbf{x}$ placed on the diagonal; $E\{\cdot\}$ denotes the statistical expectation; and finally, $\star$ denotes the linear convolution.

II. Problem Formulation

The system under investigation is an asynchronous K-user CDMA system with spreading codes of length (processing gain) N. The code waveform for user k is

$$g_k(t) = \sum_{n=0}^{N-1} c_k(n) p(t - nT_c) \tag{1}$$

where $\{c_k(n)\}_{n=0}^{N-1}$ denotes the spreading code for user k, $p(t)$ the chip waveform assumed to be *bandlimited* and identical for all users, and T_c the chip duration. The transmitted signal $\psi_k(t)$ for user k is formed by multiplying $g_k(t)$ by the mth transmitted data symbol $d_k(m)$, i.e.,

$$\psi_k(t) = \sum_{m=0}^{M-1} d_k(m) g_k(t - mT_s) \tag{2}$$

where M denotes the number of symbols used for code acquisition, and $T_s = NT_c$ denotes the symbol duration.

Consider a general scenario where the channel is both *time- and frequency-selective*. The baseband signal received at the base station can be represented as [19]

$$y'(t) = \sum_{k=1}^{K} \sum_{l=1}^{L_k} \alpha_{k,l}(t) \psi_k(t - \tau_{k,l}) + n_r(t) \tag{3}$$

where $L_k, \alpha_{k,l}(t)$, and $\tau_{k,l}$ denote the number of propagation paths, the lth path's gain, and the lth path's delay for user k, respectively, and $n_r(t)$ is the channel noise, assumed to be zero-mean with power spectral density (PSD) $N_0/2$. For ease of derivation, we assume that the time-varying fading coefficient $\alpha_{k,l}(t)$ remains (approximately) unchanged within γ symbol periods, where the integer $\gamma \geq 1$. This is reasonable since γ is usually small, e.g., $\gamma = 1$ or 2, and let

$$\alpha_{k,l}(m) \triangleq \alpha_{k,l}(t)|_{t=mT_s}. \tag{4}$$

In testing the proposed schemes, however, we will relax this assumption and allow $\alpha_{k,l}(t)$ to vary continuously according to a more realistic channel model, e.g., the Jakes' model [20]; see Section V for details.

The receiver front-end is a chip-matched filter that correlates the received signal with the chip waveform and outputs the following signal

$$\begin{aligned} y(t) &= y'(t) \star p(T_c - t) \\ &= \sum_{m=0}^{M-1} \sum_{k=1}^{K} \sum_{l=1}^{L_k} \alpha_{k,l}(m) d_k(m) s_k(t - mT_s - \tau_{k,l}) + n(t) \end{aligned} \tag{5}$$

where $s_k(t)$ denotes the *signature waveform* for user k obtained as a convolution between the spreading waveform $g_k(t)$ and the impulse response of the chip-matched filter

$$s_k(t) \triangleq g_k(t) \star p(T_c - t) \tag{6}$$

and the output noise $n(t) \triangleq n_r(t) \star p(T_c - t)$ is, in general, *colored* due to chip matched filtering, with *known* autocorrelation

$$r_n(\tau) = E\{n(t) n^*(t - \tau)\} = \frac{N_0}{2} p(T_c - \tau) \star p(\tau - T_c). \tag{7}$$

Let user k be of interest. The problem is to estimate the code-timing $\{\tau_{k,l}\}_{l=1}^{L_k}$ from the chip-matched filter output $y(t)$, assuming knowledge of the spreading code of only user k. In this paper, we do not address the issue of estimating L_k, which is assumed known. An estimate of L_k can be obtained by prior channel/cell measurements and/or through a model order detection scheme (e.g., [21]). For the problem of interest, we will consider solutions that are *blind*, in which case the information symbols $\{d_k(m)\}_{m=0}^{M-1}$ are assumed random and unknown, or training-assisted, whereby we will impose certain structure on the transmitted symbols $\{d_k(m)\}_{m=0}^{M-1}$ to seek improved performance.

III. Preliminaries

In this section, we discuss a unique structure of the transmitted signal in the frequency domain, which forms the basis

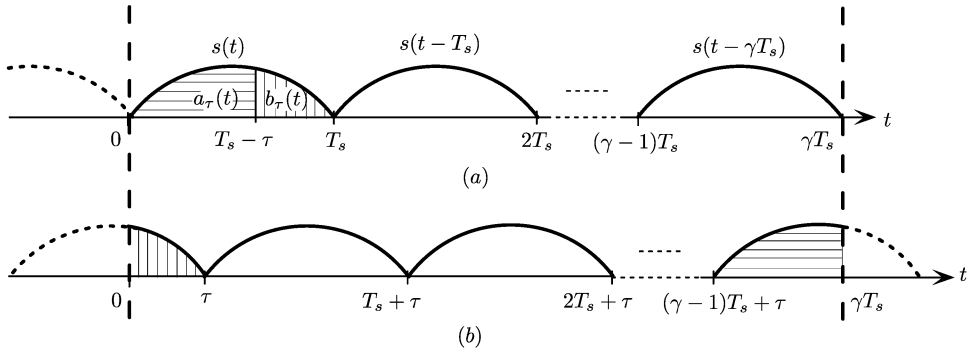

Fig. 1. Formation of the continuous-time received signal.

for all code-timing estimation schemes to be introduced in Section IV.

Consider a scenario where a set of $\gamma(\gamma \geq 1)$ adjacent symbols are processed simultaneously. It is noted that γ is a design parameter whose choice should reflect a tradeoff between complexity, estimation accuracy, and user capacity (*viz.*, how many active transmissions can be supported by the synchronization scheme). In general, the larger the γ, the better/larger the accuracy/capacity and, yet, the higher the complexity. This will become apparent in Sections IV and V. For illustration purpose, Fig. 1(a) depicts γ shifted copies of a signature waveform for one user, while Fig. 1(b) depicts a delayed version. The shape of the signature waveform is hypothetical and unimportant; what is of interest here is the relative position of the different copies of the signature waveform. Note that the signature waveform $s(t)$ is broken into two portions

$$s(t) = a_\tau(t) + b_\tau(t) \tag{8}$$

where

$$a_\tau(t) \triangleq \begin{cases} s(t) & 0 < t < T_s - \tau \\ 0 & \text{elsewhere} \end{cases}$$
$$b_\tau(t) \triangleq \begin{cases} s(t) & T_s - \tau < t < T_s \\ 0 & \text{elsewhere.} \end{cases}$$

The subscript τ signifies that both portions are functions of the unknown propagation delay τ. In the sequel, we assume that the maximum path delay is less than T_s, which can be a result of a prior coarse synchronization achieved through a side signaling channel for call setup (e.g., [4], [22]). According to the relation shown in Fig. 1, the delayed signal (with data modulation) associated with a particular user over an observation window of γT_s seconds starting at $t = mT_s$ is given by

$$\begin{aligned} x_m(t) \triangleq\ & a_\tau(t-(\gamma-1)T_s-\tau)d(m+\gamma-1) \\ & + b_\tau(t+T_s-\tau)d(m-1) \\ & + \sum_{\zeta=0}^{\gamma-2} s(t-\zeta T_s-\tau)d(m+\zeta) \end{aligned} \tag{9}$$

and note that the last term vanishes if $\gamma = 1$. To simplify the expression, we introduce the following notation

$$s^{(-1)}(t) = b_\tau(t) \tag{10}$$

$$s^{(\gamma-1)}(t) = a_\tau(t) \tag{11}$$

$$s^{(\zeta)}(t) = s(t), \quad 0 \leq \zeta \leq \gamma - 2. \tag{12}$$

Then, we can write $x_m(t)$ more compactly as follows:

$$x_m(t) = \sum_{\zeta=-1}^{\gamma-1} s^{(\zeta)}(t-\zeta T_s-\tau)d(m+\zeta). \tag{13}$$

Applying the Fourier transform to $x_m(t)$ yields[1]

$$\bar{x}_m(f) = e^{-j2\pi f\tau} \sum_{\zeta=-1}^{\gamma-1} \bar{s}^{(\zeta)}(f) e^{-j2\pi f\zeta T_s} d(m+\zeta) \tag{14}$$

where $\bar{s}^{(\zeta)}(f)$ denotes the Fourier transform of $s^{(\zeta)}(t)$. To facilitate digital signal processing, $\bar{x}_m(f)$ is sampled, i.e., via the DFT (discrete Fourier Transform), at the following equally spaced frequency grids

$$f_\mu \triangleq \mu\Delta f = \frac{\mu}{\gamma T_s}, \quad \mu = 0, 1, \ldots, \gamma NQ - 1 \tag{15}$$

where the integer $Q \geq 1$ will be referred to as *oversampling factor* (see Section IV).

A typical choice for the oversampling factor is $Q = 2$, which renders the aliasing-induced estimation error negligible. Let $\bar{s}^{(\zeta)}(\mu) \triangleq \bar{s}^{(\zeta)}(f)|_{f=\mu\Delta f}$ and $\bar{x}_m(\mu) \triangleq \bar{x}_m(f)|_{f=\mu\Delta f}$. The discrete version of (14) is given by[2]

$$\bar{x}_m(\mu) = e^{-j\frac{2\pi\mu\tau}{\gamma T_s}} \sum_{\zeta=-1}^{\gamma-1} \bar{s}^{(\zeta)}(\mu) e^{-j\frac{2\pi\mu\zeta}{\gamma}} d(m+\zeta). \tag{16}$$

Effectively, the above equation indicates that the spectrum of $x_m(t)$ defined in (13) is a complex sinusoid with a frequency proportional to the code timing τ, multiplied by a frequency function denoted by the sum in (16). The frequency function has some known structure since the spectra $\bar{s}^{(\zeta)}(\mu)$ is known for $0 \leq \zeta \leq \gamma - 2$. This observation is fundamental to the proposed code-timing estimation schemes that are to be presented in Section IV.

[1]Henceforth, $\bar{(\cdot)}$ is used to denote quantities in the frequency domain.

[2]DFT will incur some frequency-domain aliasing that diminishes with increasing sampling frequency. Assuming slight oversampling (e.g., at twice the chip rate), the aliasing-induced estimation error is in general negligible compared to the error caused by channel noise and MAI inherent in CDMA systems; see, e.g., [23].

We will consider in the sequel two approaches, namely blind and training-assisted techniques, to solve the code-timing estimation problem. For blind estimation, we will model the information symbols, which appear in the sum in (16), as *unknown* and *random*. For training-based estimation, we will impose an additional constraint that the training symbols for the desired user are identical. Assuming without loss of generality *all-one* training, it is straightforward to show that (16) reduces to

$$\begin{aligned}\bar{x}_m(\mu) &= \bar{s}(\mu)e^{-j\frac{2\pi\mu\tau}{\gamma T_s}}\sum_{\zeta=0}^{\gamma-1}e^{-j\frac{2\pi\mu\zeta}{\gamma}} \\ &= \bar{s}(\mu)e^{-j\frac{2\pi\mu\tau}{\gamma T_s}}\frac{1-e^{-j2\pi\mu}}{1-e^{-j\frac{2\pi\mu}{\gamma}}} \\ &= \gamma\bar{s}(\mu)e^{\frac{-j2\pi\mu\tau}{\gamma T_s}}\delta_{\mu,n\gamma} \\ &\qquad n=0,1,\ldots,NQ-1 \quad (17)\end{aligned}$$

where $\delta_{i,j}$ denotes the Kronecker delta, $\bar{s}(\mu) \triangleq \bar{s}(f)|_{f=\mu\Delta f}$, with $\bar{s}(f)$ denoting the Fourier transform of $s(t)$, and we have used the fact that

$$e^{j\frac{2\pi\mu}{\gamma}} = e^{-j\frac{2\pi(\gamma-1)\mu}{\gamma}} \quad (18)$$

$$\bar{s}(\mu) = \bar{s}^{(-1)}(\mu) + \bar{s}^{(\gamma-1)}(\mu). \quad (19)$$

Equation (17) can, again, be interpreted as a complex sinusoid with a frequency proportional to τ multiplied by a frequency function. The complex sinusoid is upsampled by a factor of γ (without interpolation) [24]. We stress that the frequency function in the current case is completely known to the receiver, while in the former blind case, it is in general unknown since it depends on the unknown symbols and, furthermore, the spectra $\bar{s}^{(-1)}(\mu)$ and $\bar{s}^{(\gamma-1)}(\mu)$ are functions of the unknown delay τ [cf. (10)–(11)]. This will lead to different performance of the proposed training-based and blind code-timing estimation schemes, as we shall see later.

IV. Blind and Training-Assisted Code-Timing Estimation

In this section, we present both blind and training-based subspace solutions to the problem of interest. Since both are frequency-domain based schemes, we first discuss the DFT-converted signal in vector form in the frequency domain. We then present the proposed blind and training-assisted subspace code-timing estimation algorithms. Following our detailed treatment of the blind schemes, our discussions on the training-assisted methods are brief, focusing on the difference from the former.

We will process γ adjacent symbols from the output (5) of the chip-matched filter. To this end, we form overlapping signals $y_m(t)$ of duration μT_s as

$$y_m(t) = \begin{cases} y(t), & mT_s \le t \le (m+\gamma)T_s \\ 0, & \text{otherwise.}\end{cases}$$

Using the notation introduced in Section III, $y_m(t)$ can be expressed as

$$\begin{aligned}y_m(t) = \sum_{k=1}^{K}\sum_{l=1}^{L_k}\alpha_{k,l}(m)\sum_{\zeta=-1}^{\gamma-1}s_k^{(\zeta)}(t-mT_s-\zeta T_s-\tau_{k,l}) \\ \times d_k(m+\zeta)+n(t)\end{aligned}$$

where $s_k^{(\zeta)}(t)$ is similarly defined as in (10)–(12) for user k and delay $\tau_{k,l}$. Note that for $\tau_{k,l} < T_s$, the observation window covering M symbols is $(M+1)T_s$. It follows that the number of overlapping signals is equal to $M-\gamma+2$.

For DSP processing, $y_m(t)$ is sampled with a sampling interval $T_i = T_c/Q$:

$$y_m(i) = y_m(t)|_{t=mT_s+iT_i}, \quad i=0,1,\ldots,\gamma NQ-1 \quad (20)$$

where the $Q \ge 1$ is referred to as *oversampling factor*. A typical choice for the oversampling factor is $Q=2$, which renders the aliasing-induced estimation error negligible [23]. Let

$$\begin{aligned}\mathbf{y}(m) \triangleq [y_m(mNQ),\ldots,y_m(mNQ+\gamma NQ-1)]^T \\ m=0,1,\ldots,M-\gamma+1.\end{aligned}$$

As mentioned in Section III, different choices of γ lead to different code-timing estimators, with different tradeoffs in accuracy, capacity, and complexity. Let $\mathbf{n}(m)$ be $\gamma NQ \times 1$ vector formed similarly from the noise samples, and

$$\begin{aligned}\mathbf{s}_k^{(\zeta)}(\tau_{k,l}) \triangleq \Big[s_k^{(\zeta)}(-\zeta NQ-\tau_{k,l}),\ldots, \\ s_k^{(\zeta)}((\gamma-\zeta)NQ-1-\tau_{k,l})\Big]^T \\ \zeta=-1,0,\ldots,\gamma-1 \quad (21)\end{aligned}$$

which consist of samples of the delayed signature waveforms. In vector form, the received signal can be written as

$$\mathbf{y}(m) = \sum_{k=1}^{K}\sum_{l=1}^{L_k}\sum_{\zeta=-1}^{\gamma-1}\beta_{k,l}(m+\zeta)\mathbf{s}_k^{(\zeta)}(\tau_{k,l}) + \mathbf{n}(m) \quad (22)$$

where

$$\beta_{k,l}(m) \triangleq \alpha_{k,l}(m)d_k(m). \quad (23)$$

It is assumed that the channel remains approximately unchanged within a period of γ symbol periods such that $\alpha_{k,l}(m+\zeta) = \alpha_{k,l}(m), \zeta = -1,\ldots,\gamma-1$. This assumption is reasonable since γ is usually small, e.g., $\gamma = 1$ or 2. Again, the assumption is mainly for the sake of simplicity of derivation. We will drop the assumption in our simulation and consider continuously fading channels according to the Jakes' model; see Section V. Recall that after chip-matched filtering, $\mathbf{n}(m)$ is colored with covariance matrix $\mathbf{R}_n \triangleq E\{\mathbf{n}(m)\mathbf{n}^H(m)\}$ formed by samples of the autocorrelation function (7) that is known to the receiver.

To convert the signal to the frequency domain, we take the DFT of the observed vectors $\mathbf{y}(m)$. Before proceeding, a few remarks are necessary. It is noted that the spectrum of a typical bandlimited signature waveform usually tapers off at the end (i.e., high) frequencies. To see this, Fig. 2 depicts the magnitude spectrum of a signature waveform as a function of the normalized frequency fT_c. The signature waveform is formed by using a square-root raised-cosine chip waveform and a Gold spreading code with processing gain $N = 31$. It is clearly seen that the signature waveform has a low-pass nature, with the magnitude spectrum tapering off quickly as the frequency increases (e.g., $f > 1/(2T_c)$ in Fig. 2). In the presence of channel noise, which typically has a wider spectrum than the signal bandwidth, the end frequencies have a lower signal-to-noise ratio (SNR) than

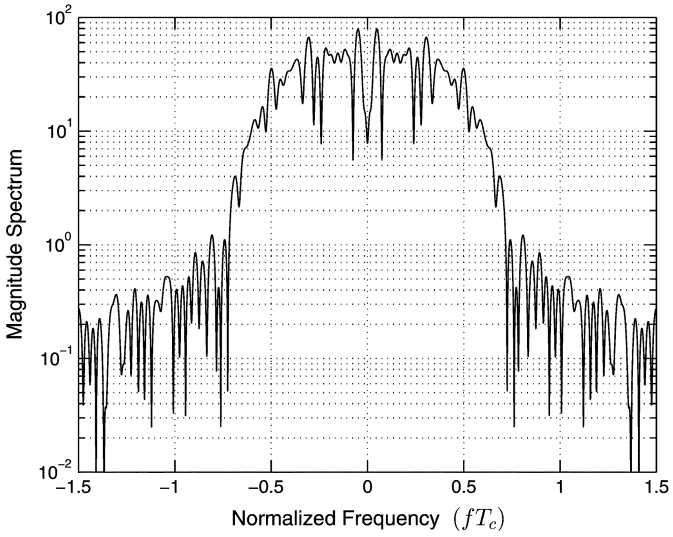

Fig. 2. Magnitude spectrum of a typical spreading waveform $s_k(t)$.

the middle frequencies. In view of this observation, we shall discard the low-SNR end DFT grids, keeping only the high-SNR middle DFT grids for delay estimation (also see [23] for a discussion). To do so, we can utilize $\eta \in (0, 1]$ as a DFT grid selection parameter. Consider the following $\gamma N_s \times \gamma NQ$ *truncated* DFT matrix

$$\mathcal{F} = \begin{bmatrix} 1 & 1 & \cdots & 1 \\ 1 & e^{-j\frac{2\pi}{\gamma NQ}} & \cdots & e^{-j\frac{2\pi}{\gamma NQ}(\gamma NQ-1)} \\ \vdots & \vdots & \vdots & \vdots \\ 1 & e^{-j\frac{2\pi}{\gamma NQ}(\gamma N_s-1)} & \cdots & e^{-j\frac{2\pi}{\gamma NQ}(\gamma N_s-1)(\gamma NQ-1)} \end{bmatrix}$$

which is formed by the γN_s rows corresponding to the selected middle DFT grids of the $\gamma NQ \times \gamma NQ$ full DFT matrix, where $N_s = \lceil \eta NQ \rceil$, with $\lceil \cdot \rceil$ denoting the smallest integer no less than the argument. Let

$$\bar{\mathbf{y}}(m) \triangleq \mathcal{F}\mathbf{y}(m) \tag{24}$$

$$\bar{\mathbf{s}}_k^{(\zeta)}(\tau_{k,l}) \triangleq \mathcal{F}\mathbf{s}_k^{(\zeta)}(\tau_{k,l}). \tag{25}$$

It is easy to see that $\mathcal{F}\mathbf{x}$ for any $\gamma NQ \times 1$ vector $\mathbf{x}$ is equivalent to computing a full-grid DFT of $\mathbf{x}$ followed by discarding the unwanted DFT samples. Since a full-grid DFT can be efficiently computed by fast Fourier transform (FFT), the matrix multiplication is never needed for implementation; $\mathcal{F}$ is introduced only for analysis. Finally, we remark that a typical choice of η is between 0.5 and 0.9.

The DFT-converted signal can be written as

$$\bar{\mathbf{y}}(m) = \sum_{k=1}^{K}\sum_{l=1}^{L_k}\sum_{\zeta=-1}^{\gamma-1} \beta_{k,l}(m+\zeta)\bar{\mathbf{s}}_k^{(\zeta)}(\tau_{k,l}) + \bar{\mathbf{n}}(m) \qquad m = 0, 1, \ldots, M-\gamma+1 \tag{26}$$

where $\bar{\mathbf{n}}(m) \triangleq \mathcal{F}\mathbf{n}(m)$, which is colored with covariance matrix

$$\mathbf{R}_{\bar{n}} \triangleq E\{\bar{\mathbf{n}}(m)\bar{\mathbf{n}}^H(m)\} = \mathcal{F}\mathbf{R}_n\mathcal{F}^H. \tag{27}$$

Applying prewhitening, we have

$$\tilde{\mathbf{y}}(m) \triangleq \mathbf{R}_{\bar{n}}^{-1/2}\bar{\mathbf{y}}(m) = \sum_{k=1}^{K}\sum_{l=1}^{L_k}\sum_{\zeta=-1}^{\gamma-1} \beta_{k,l}(m+\zeta)\tilde{\mathbf{s}}_k^{(\zeta)}(\tau_{k,l}) + \tilde{\mathbf{n}}(m) \tag{28}$$

where

$$\tilde{\mathbf{s}}_k^{(\zeta)}(\tau_{k,l}) \triangleq \mathbf{R}_{\bar{n}}^{-1/2}\bar{\mathbf{s}}_k^{(\zeta)}(\tau_{k,l}) \tag{29}$$

$$\tilde{\mathbf{n}}(m) \triangleq \mathbf{R}_{\bar{n}}^{-1/2}\bar{\mathbf{n}}(m). \tag{30}$$

It is easy to see that $\tilde{\mathbf{n}}(m)$ is spectrally white with identity covariance matrix.

The blind and training-based code-timing estimation schemes to be introduced next all rely on the subspace structure of $\text{span}\{\tilde{\mathbf{y}}(0), \ldots, \tilde{\mathbf{y}}(M-\gamma+1)\}$, which can be decomposed into a signal and a noise subspace that are orthogonal to one another. The signal subspace is spanned by signal vectors $\tilde{\mathbf{s}}_k^{(\zeta)}(\tau_{k,l})$ for all k, l, and ζ. A number of observations regarding these vectors are in order.

- The signature vectors $\mathbf{s}_k^{(\zeta)}(\tau_{k,l})$ are linearly independent for different k since different users have linearly independent spreading codes.
- For the same $k, \mathbf{s}_k^{(\zeta)}(\tau_{k,l})$ are linearly independent for different l since different paths have distinct delays.
- DFT and whitening do not change the linear independence structure.

Therefore, $\tilde{\mathbf{s}}_k^{(\zeta)}(\tau_{k,l})$ are linearly independent of each other, a property that is needed for proper subspace decomposition and identification.

A. Blind Estimation

For blind estimation, the receiver is unaware of the user information symbols $d_k(m)$, which can in general be modeled as independent in m (time) and k (user). Furthermore, the fading coefficients $\alpha_{k,l}(m)$, which are modeled as stationary random processes, are assumed independent of the information symbols. Under these conditions, we have

$$\mathbf{R}_{\tilde{y}} \triangleq E\{\tilde{\mathbf{y}}(m)\tilde{\mathbf{y}}^H(m)\} = \sum_{k=1}^{K}\sum_{l=1}^{L_k}\sum_{\zeta=-1}^{\gamma-1} P_{k,l}\tilde{\mathbf{s}}_k^{(\zeta)}(\tau_{k,l})\tilde{\mathbf{s}}_k^{(\zeta)H}(\tau_{k,l}) + \mathbf{I} \tag{31}$$

where $P_{k,l} \triangleq E\{|\beta_{k,l}(m)|^2\} = E\{|\alpha_{k,l}(m)|^2\}$, assuming that the information symbols are drawn from a unit-energy constellation. Let

$$L \triangleq \sum_{k=1}^{K} L_k. \tag{32}$$

According to our previous discussion about the linear independence of $\{\tilde{\mathbf{s}}_k^{(\zeta)}(\tau_{k,l})\}$, the eigenvalue decomposition of $\mathbf{R}_{\tilde{y}}$ can be written as

$$\mathbf{R}_{\tilde{y}} = \mathbf{E}_s\mathbf{\Lambda}_s\mathbf{E}_s^H + \mathbf{E}_n\mathbf{E}_n^H \tag{33}$$

where $\mathbf{\Lambda}_s$ is a diagonal matrix formed by the $(\gamma+1)L$ largest eigenvalues, $\mathbf{E}_s \in \mathbb{C}^{\gamma N_s \times (\gamma+1)L}$ spans the $(\gamma+1)L$-dimen-

sional signal subspace, $\mathbf{E}_n \in \mathbb{C}^{\gamma N_s \times [\gamma N_s - (\gamma+1)L]}$ spans the $[\gamma N_s - (\gamma+1)L]$-dimensional noise subspace that is orthogonal to $\mathbf{E}_s$. It follows that

$$\mathbf{E}_n^H \tilde{\mathbf{s}}_k^{(\zeta)}(\tau_{k,l}) = \mathbf{0}, \quad \zeta = -1, 0, \ldots, \gamma - 1. \tag{34}$$

Hence, we have a set of $\gamma + 1$ equations that can be used to estimate the unknown delay. The remaining question is how to solve these equations efficiently, which is addressed next.

We first express $\tilde{\mathbf{s}}_k^{(\zeta)}(\tau_{k,l})$ explicitly as a function of $\tau_{k,l}$. Recall that $\mathbf{s}_k^{(\zeta)}(\tau_{k,l})$ is formed by samples of the linearly shifted signature waveforms $s_k^{(\zeta)}(\tau_{k,l})$ [see (21)]. Let $\mathbf{s}_k^{(\zeta)}$ be formed by samples of $s_k^{(\zeta)}(t)$, with proper zero-padding to make it a $\gamma NQ \times 1$ vector, and

$$\bar{\mathbf{s}}_k^{(\zeta)} \triangleq \mathcal{F}\mathbf{s}_k^{(\zeta)}. \tag{35}$$

By the shifting property of Fourier transform, we have [also see (16)]

$$\tilde{\mathbf{s}}_k^{(\zeta)}(\tau_{k,l}) = \mathbf{R}_{\bar{n}}^{-1/2} \boldsymbol{\Theta}^{\zeta} \bar{\mathbf{S}}_k^{(\zeta)} \boldsymbol{\phi}(\tau_{k,l}) \tag{36}$$

where

$$\bar{\mathbf{S}}_k^{(\zeta)} = \operatorname{diag}\left\{\bar{\mathbf{s}}_k^{(\zeta)}\right\} \tag{37}$$

$$\boldsymbol{\Theta} = \operatorname{diag}\left\{1, e^{-j\frac{2\pi}{\gamma}}, \ldots, e^{-j\frac{2\pi(\gamma N_s - 1)}{\gamma}}\right\} \tag{38}$$

$$\boldsymbol{\phi}(\tau_{k,l}) = \left[1, e^{-j\frac{2\pi\tau_{k,l}}{\gamma T_s}}, \ldots, e^{-j\frac{2\pi\tau_{k,l}(\gamma N_s - 1)}{\gamma T_s}}\right]^T. \tag{39}$$

Substituting (36) into (34), we have

$$\mathbf{E}_n^H \mathbf{R}_{\bar{n}}^{-1/2} \boldsymbol{\Theta}^{\zeta} \bar{\mathbf{S}}_k^{(\zeta)} \boldsymbol{\phi}(\tau_{k,l}) = \mathbf{0}, \quad \zeta = -1, 0, \ldots, \gamma - 1. \tag{40}$$

Note that all $\bar{\mathbf{S}}_k^{(\zeta)}, 0 \le \zeta \le \gamma - 2$, are known to the receiver, except $\bar{\mathbf{S}}_k^{(-1)}$ and $\bar{\mathbf{S}}_k^{(\gamma-1)}$, which depend on the unknown parameter $\tau_{k,l}$ [see (10)–(12)]. The two equations in (40) involving $\bar{\mathbf{S}}_k^{(-1)}$ and $\bar{\mathbf{S}}_k^{(\gamma-1)}$ are highly nonlinear and, therefore, difficult to solve. If $\gamma \ge 2$, one possible approach is to discard these two and use the other $\gamma - 1$ equations to estimate τ. However, we do not recommend so since better performance is expected by exploiting all $\gamma + 1$ equations for estimation.

To cope with the above difficulty, we note that since $\mathbf{E}_n$ is orthogonal to the signal subspace, it is also orthogonal to any linear combination of the signal vectors. Summing all $\gamma + 1$ equations in (40) yields

$$\begin{aligned}
\mathbf{0} &= \mathbf{E}_n^H \mathbf{R}_{\bar{n}}^{-1/2} \sum_{\zeta=-1}^{\gamma-1} \boldsymbol{\Theta}^{\zeta} \bar{\mathbf{S}}_k^{(\zeta)} \boldsymbol{\phi}(\tau_{k,l}) \\
&= \mathbf{E}_n^H \mathbf{R}_{\bar{n}}^{-1/2} \left[\boldsymbol{\Theta}^{-1} \bar{\mathbf{S}}_k^{(-1)} + \boldsymbol{\Theta}^{\gamma-1} \bar{\mathbf{S}}_k^{(\gamma-1)} \right. \\
&\quad \left. + \left(\sum_{\zeta=0}^{\gamma-2} \boldsymbol{\Theta}^{\zeta}\right) \bar{\mathbf{S}}_k \right] \boldsymbol{\phi}(\tau_{k,l}) \\
&= \mathbf{E}_n^H \mathbf{R}_{\bar{n}}^{-1/2} \left[\boldsymbol{\Theta}^{\gamma-1} \bar{\mathbf{S}}_k + \left(\sum_{\zeta=0}^{\gamma-2} \boldsymbol{\Theta}^{\zeta}\right) \bar{\mathbf{S}}_k \right] \boldsymbol{\phi}(\tau_{k,l}) \\
&= \mathbf{E}_n^H \mathbf{R}_{\bar{n}}^{-1/2} \bar{\boldsymbol{\Theta}} \bar{\mathbf{S}}_k \boldsymbol{\phi}(\tau_{k,l})
\end{aligned} \tag{41}$$

where in the second equality we dropped the superscript ζ of $\bar{\mathbf{S}}_k^{(\zeta)}$ for $0 \le \zeta \le \gamma - 2$,[3] in the third equality, we used the fact that [cf. (18)–(19)]

$$\boldsymbol{\Theta}^{-1} = \boldsymbol{\Theta}^{\gamma-1} \tag{42}$$

$$\bar{\mathbf{S}}_k^{(-1)} + \bar{\mathbf{S}}_k^{(\gamma-1)} = \bar{\mathbf{S}}_k \tag{43}$$

and finally, $\bar{\boldsymbol{\Theta}}$ is a $\gamma N_s \times \gamma N_s$ diagonal matrix that is known to the receiver

$$\bar{\boldsymbol{\Theta}} \triangleq \sum_{\zeta=0}^{\gamma-1} \boldsymbol{\Theta}^{\zeta}. \tag{44}$$

Note that all terms except $\boldsymbol{\phi}(\tau)$ on the right-hand side (last step) of (41) are now independent of τ. Solving (41) for τ becomes immediate. In particular, define a frequency parameter that is linearly related to the delay

$$f_{k,l} \triangleq -\frac{\tau_{k,l}}{\gamma T_s}. \tag{45}$$

The delay estimation problem is equivalent to estimating frequency $f_{k,l}$, which can be obtained through a polynomial rooting procedure ([25, p. 158]). Specifically, let

$$z \triangleq e^{-j2\pi f_{k,l}} \tag{46}$$

$$\boldsymbol{\phi}(z) \triangleq \left[1, z, \ldots, z^{(\gamma N_s - 1)}\right]^T. \tag{47}$$

Then, (41) can be written as

$$\boldsymbol{\phi}^T(z^{-1}) \bar{\mathbf{S}}_k^H \bar{\boldsymbol{\Theta}}^H \mathbf{R}_{\bar{n}}^{-1/2} \mathbf{E}_n \mathbf{E}_n^H \mathbf{R}_{\bar{n}}^{-1/2} \bar{\boldsymbol{\Theta}} \bar{\mathbf{S}}_k \boldsymbol{\phi}(z) = 0. \tag{48}$$

One can quickly see that the left-hand side (LHS) of the above equation is a polynomial in z. The polynomial has a root located on the unit circle and the phase of the root is $-2\pi f_{k,l}$. Hence, the frequency $f_{k,l}$ can be estimated by rooting the polynomial and identify the phase of the unit-amplitude root. A multitude of good polynomial rooting algorithms are available (see [26], [27], and references therein). The computational complexity aspect of polynomial rooting based algorithms is addressed in [25, Sect. 4.5].

Remark 1: The earlier discussion was focused on the case in which the code timing of a single path is to be found. When there are L_k propagation paths associated with user k, the polynomial (48) has L_k roots on the unit circle.

Remark 2: A necessary condition for the proposed technique is that the noise subspace spanned by $\mathbf{E}_n$ is nontrivial. This requires that $\gamma N_s > (\gamma+1)L$ or, equivalently, $\gamma > L/(N_s - L)$ provided that $N_s > L$. Recall that L defined in (32) is related to the number of users in the system. Hence, the choice of γ has a direct impact on the user capacity. As we shall see in Section V, choosing a larger γ also leads to improved estimation accuracy given the same number of users in the system. As such we refer to the proposed blind technique for different γ as a group of estimators. The complexity of the proposed estimators grows with increasing γ because vectors of larger dimensions are utilized, which invovles eigendecomposition of larger covariance matrices.

[3]Note that $\bar{\mathbf{s}}_k^{(\zeta)}$ defined in (35) are independent of ζ for $0 \le \zeta \le \gamma - 2$; see (12).

Remark 3: The true covariance matrix $\mathbf{R}_{\tilde{y}}$ used for eigendecomposition is unknown, and has to be replaced by some estimate, such as the sample covariance matrix

$$\hat{\mathbf{R}}_{\tilde{y}} = \frac{1}{M-\gamma+2} \sum_{m=0}^{M-\gamma+1} \tilde{\mathbf{y}}(m)\tilde{\mathbf{y}}^H(m). \tag{49}$$

The noise eigenvectors $\hat{\mathbf{E}}_n$ based on the eigendecomposition of the noisy $\hat{\mathbf{R}}_{\tilde{y}}$, in general, are only approximately orthogonal to the signal vectors $\tilde{\mathbf{s}}_k^{(\zeta)}(\tau_{k,l})$. As a result, (41) holds approximately and needs to be solved in the least-squares (LS) sense. Likewise, (48) generally does not have L_k roots *exactly* on the unit circle. Instead, we can utilize those roots that are closest to the unit circle.

The proposed blind schemes, as well as the training-based ones to be discussed next, assume knowledge of the number of users and the number of paths of each user. For the reverse link considered in this paper, the base station has knowledge of the number of users in the system, but needs to estimate the number of paths. Path estimation belongs to the general model structure selection problem, and a multitude of good methods can be used to solve the problem (see [28]). Since these methods are subject to estimation errors, we consider via simulations in Section V the impact of inaccurate path estimation on the proposed code-timing estimation schemes.

B. Training-Based Estimation

While the proposed blind code-timing estimation schemes require no knowledge of the information symbols, we can improve the performance by transmitting known training symbols for the desired user. Without loss of generality, let the first user be the desired one. The training symbols are assumed identical: $d_1(m) = 1, \forall m$. Taking into account of the special training sequence, we isolate the desired user from the others and rewrite (28) as follows:

$$\begin{aligned}\tilde{\mathbf{y}}(m) &= \sum_{l=1}^{L_1} \alpha_{1,l}(m) \sum_{\zeta=-1}^{\gamma-1} \tilde{\mathbf{s}}_1^{(\zeta)}(\tau_{1,l}) \\ &\quad + \sum_{k=2}^{K} \sum_{l=1}^{L_k} \sum_{\zeta=-1}^{\gamma-1} \beta_{k,l}(m+\zeta)\tilde{\mathbf{s}}_k^{(\zeta)}(\tau_{k,l}) + \tilde{\mathbf{n}}(m) \\ &= \mathbf{R}_{\tilde{n}}^{-1/2}\bar{\mathbf{\Theta}}\bar{\mathbf{S}}_k \sum_{l=1}^{L_1} \alpha_{1,l}(m)\boldsymbol{\phi}(\tau_{k,l}) \\ &\quad + \sum_{k=2}^{K} \sum_{l=1}^{L_k} \sum_{\zeta=-1}^{\gamma-1} \beta_{k,l}(m+\zeta)\tilde{\mathbf{s}}_k^{(\zeta)}(\tau_{k,l}) + \tilde{\mathbf{n}}(m). \end{aligned} \tag{50}$$

A few remarks on the above equation are in order. First, $\beta_{1,l}(m)$ for user one reduces to $\alpha_{1,l}(m)$ due to all-one training [see (23)]. Second, it is assumed that the channel remains approximately unchanged within a period of γ symbol periods such that $\alpha_{1,l}(m+\zeta) = \alpha_{1,l}(m), \zeta = -1, \ldots, \gamma-1$. As we mentioned earlier in this section, this assumption is reasonable since γ is usually small. We will drop the assumption in our simulation and consider continuously fading channels according to the Jakes' model; see Section V. Finally, the second equality of (50) follows similar steps in (41) for user one.

It is noted that we did not try to simplify the expressions for the other interfering user signals in (41). This is because with their information symbols unknown and random, they take similar forms as in the former blind case in Section IV.A. In particular, each propagation path of these interfering users contributes $\gamma+1$ independent vectors to the signal subspace; on the other hand, *each propagation path for the desired user only contributes one vector to the signal subspace*. In view of this difference, one can see that although the eigendecomposition of the covariance matrix of $\mathbf{R}_{\tilde{y}}$ in the current case takes the same form as in (33), the signal/noise subspaces involve different dimensions. In particular, we now have $\mathbf{E}_s \in \mathbb{C}^{\gamma N_s \times [(\gamma+1)(L-L_1)+L_1]}$ spans the $[(\gamma+1)(L-L_1)+L_1]$-dimensional signal subspace, and $\mathbf{E}_n \in \mathbb{C}^{\gamma N_s \times [\gamma N_s - (\gamma+1)(L-L_1)-L_1]}$ spans the $[\gamma N_s - (\gamma+1)(L-L_1)-L_1]$-dimensional noise subspace that is orthogonal to $\mathbf{E}_s$. Once the noise subspace is properly identified from the eigendecomposition of $\mathbf{R}_{\tilde{y}}$, the remaining steps of the training-based scheme for a particular γ is the same as in the blind scheme with the same γ. Again, we stress that we have a group of training-assisted schemes with different γ because they offer different tradeoffs in accuracy, capacity, and complexity, similar to the blind estimation case.

Remark 4: To summarize, the proposed training-based code-timing estimation methods involve transmission of identical training symbols for the desired user. The associated noise subspace has a larger dimension than its counterpart for the blind case. Other than such differences, implementations of the training-based and blind schemes are identical for the same choice of γ. The difference in subspace dimension, however, does lead to different performance of the two categories of algorithms, as will be seen in the next section.

V. Numerical Results

We consider a K-user asynchronous DS-CDMA system using a unit-energy binary phase shift keying (BPSK) constellation and a square-root raised-cosine chip pulse with roll-off factor equal to one [15]. The pulse is truncated to a duration of $4T_c$ [23]. Each user is assigned an $N = 31$ Gold code consisting of 1 and -1. To model both small- and large-scale fading, we decompose the fading coefficient into two parts and generate them separately: $\alpha_{k,l}(iT_i) = \xi_{k,l}(iT_i)P_{k,l}$, where T_i denotes the sampling interval [cf. (20)], $\xi_{k,l}(iT_i)$ is a zero-mean, unit-variance complex Gaussian random variable modeling the small-scale time-varying Rayleigh fading (more discussion later), while $P_{k,l}$ follows a log normal distribution to emulate the large-scale path loss and shadowing [22]. In the sequel, we consider near-far environments without enforcing stringent power control, where the total (from all paths) average power for the desired user is scaled so that $P_1 \triangleq \sum_{l=1}^{L_1} P_{1,l} = 1$, while the power for the $K-1$ interfering users follows a log normal distribution with a mean power $\bar{P}$ dB higher than that of the desired user. The near-far ratio (NFR) is defined as $\bar{P}$ (in dB). The SNR used below is SNR per bit.

We consider both *time-* and *frequency-selective* channel fading channels that are generated according to the Jakes' model [20]. In particular, the fading process $\xi_{k,l}(iT_i)$ has the classical U-shaped PSD and unit power, parameterized by the

normalized Doppler rate $f_D T_s$, where f_D is the maximum Doppler rate and T_s the symbol interval. In our simulations, the fading process is generated according to the Jakes' model and updated continuously every T_i seconds. As a result, the fading does not remain unchanged within a symbol interval as assumed in our earlier derivation.

In what follows, we simulate and assess the performance of the proposed blind and training-assisted schemes with two choices of the design parameters, namely $\gamma = 1$ and $\gamma = 2$, respectively. We also compare our schemes with a matched-filter (MF) scheme (e.g., [2, ch. 5]), which is also implemented in the frequency domain with all-one training for the desired user, and the time-subspace (TS) scheme proposed by Östman and Ottersten [16] that was also designed for bandlimited chip waveforms. For brevity, our schemes will be referred to as the *FS-blind* or *FS-trained* schemes, with FS standing for frequency subspace, whereas the scheme of [16] is likewise called the TS. The TS scheme requires initial parameter estimates, which are provided by the original subspace scheme of [7] for rectangular pulses, followed by nonlinear iterative searches over the parameter space. The shift-invariance based scheme of [17] is not considered here since it is not designed for time- and frequency-selective channels.

The primary performance measure adopted here is the *probability of correct acquisition*, defined as the probability of the event that the delay estimate is within a half chip of the true delay. Another performance measure is the root-mean-squared error (rmse), normalized by T_c, of the delay estimate given correct acquisition. In the multipath case, we evaluate the probability of acquisition for each path regardless of the acquisition of the other paths, then, the *averaged* probability of acquisition for all paths is considered. This implies that if correct acquisition is achieved with only a single path, the overall performance would still be very poor (due to averaging with paths with incorrect acquisition). The rmse results are reported in a similar fashion. All results shown below are based on hundreds of Monte Carlo trials, where the over-sampling factor $Q = 2$ and $\tau_{k,l}$ (delay), $\xi_{k,l}$ (small-scale fading), $P_{k,l}$ (large-scale fading) for $k \neq 1, d_k(m)$ (except $d_1(m) \equiv 1$ for the training-assisted schemes) and channel noise are varied independently from trial to trial. Unless otherwise specified, the DFT grid selection parameter is $\eta = 1$ for the proposed techniques.

Fig. 3(a) and (b) depict the probability of correct acquisition and rmse, respectively, of the proposed FS, TS, and MF methods as a function of the number of user K (user capacity) in time-varying frequency-selective Rayleigh-fading channels when $M = 150, \mathrm{SNR} = 20$ dB, $\mathrm{NFR} = 10$ dB, $f_D T_s = 0.01$, and $L_k = 2, \forall k$. It is seen that the proposed schemes outperform the time-subspace method and the MF in terms of both probability of acquisition and rmse. It is seen that the performance of the MF is limited in the multipath multiuser environment. The poor performance of the TS scheme is due to inaccurate initial parameter estimates provided by the scheme of [7], which assumes that the chip waveform is rectangular. On the other-hand, it can be seen from Fig. 3(a) that the TS scheme outperforms the FS $(\gamma = 1)$ schemes for large number of users $(K \geq 11)$. This is because FS discards the tail frequency samples (i.e., $\eta < 1$), which reduces the dimension of the noise subspace. As K increases, the number of independent noise eigenvectors decreases, which has an negative impact on both TS and FS $(\gamma = 1)$. The latter is affected more because there are fewer number of noise eigenvectors available for estimation, due to discarding the tail frequency samples. Increasing γ from 1 to 2 can improve significantly the user capacity as well as estimation accuracy. It is also observed from Fig. 3(a) and (b) that the proposed training-assisted schemes outperform the blind ones (for the same value of γ), which is not surprising since the former utilize more information about the transmission.

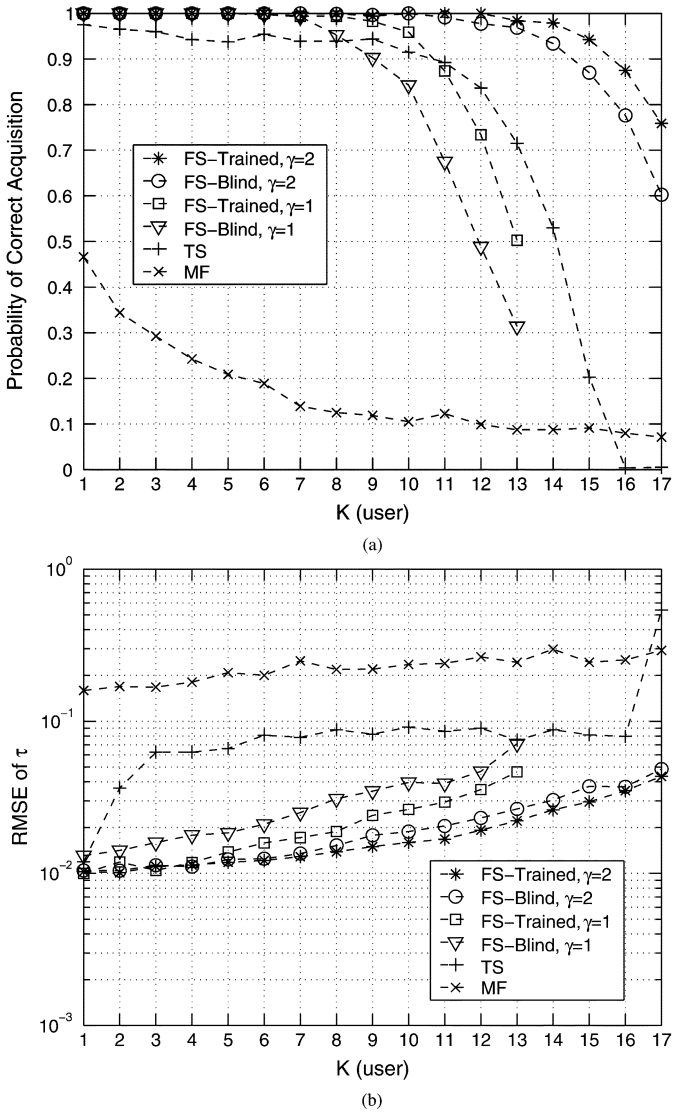

Fig. 3. Performance versus the number of users K in time-varying frequency-selective fading channels when $Q = 2, M = 150, \mathrm{SNR} = 20$ dB, $\mathrm{NFR} = 10$ dB, $f_D T_s = 0.01$, and $L_k = 2, \forall k$. (a) Probability of correct acquisition. (b) rmse.

Fig. 4(a) and (b) shows the performance of the three methods as a function of the SNR in time-varying two-path Rayleigh-fading channels when $M = 150, K = 6, \mathrm{NFR} = 10$ dB, and $f_D T_s = 0.01$. Also shown in Fig. 4(b) is the unconditional CRB derived in [29]. Since the CRB depends on the propagation delays, in this example they are randomly generated and then fixed through the simulation, whereas the other parameters are changed randomly from one trial to another. In terms of acquisition, it is seen from Fig. 4(a) that the proposed schemes

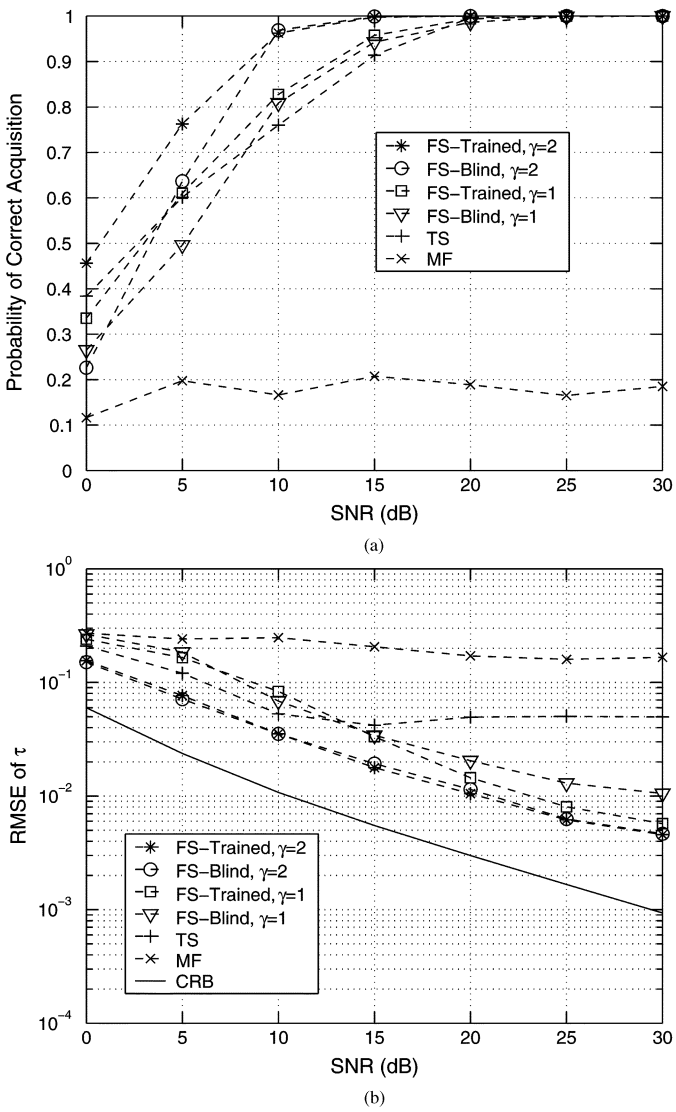

Fig. 4. Performance versus SNR in time-varying frequency-selective fading channels when $Q = 2, M = 150, K = 6, \mathrm{NFR} = 10$ dB, $f_D T_s = 0.01$, and $L_k = 2, \forall k$. (a) Probability of correct acquisition. (b) rmse.

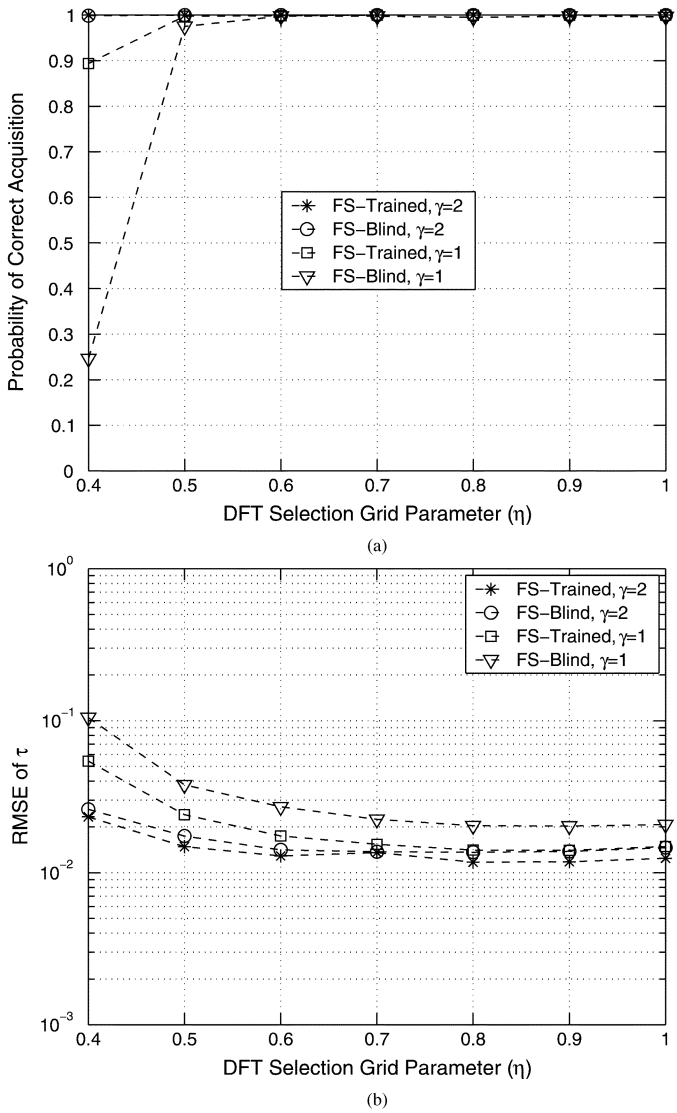

Fig. 5. Performance versus the DFT selection grid parameterη in time-varying frequency-selective fading channels when $Q = 2, K = 6, \mathrm{NFR} = 10$ dB, $\mathrm{SNR} = 20$ dB, $M = 150, f_D T_s = 0.01$, and $L_k = 2, \forall k$. (a) Probability of correct acquisition. (b) rmse.

have the smallest SNR threshold. Fig. 4(b) indicates that the proposed schemes are also more consistent than the others. That is, the estimation error of the former decreases consistently as the SNR increases, whereas the other two exhibit irreducible error floors.

We next examine numerically the choice of η, the DFT grid selection parameter (see Section IV), for the proposed schemes. Fig. 5(a) and (b) depict the probability of correct acquisition and rmse, respectively, of the proposed schemes in time-varying two-path Rayleigh-fading channels when $M = 150, \mathrm{NFR} = 10$ dB, $\mathrm{SNR} = 20$ dB, $K = 6$ and $f_D T_s = 0.01$. It is seen that as η increases, the performance of the proposed schemes improves; when η is too large (i.e., close to one), however, the estimation accuracy suffers slightly [cf. Fig. 5(b)], due to the inclusion of noisy end DFT grids. We note that in testing the algorithms versus η for $Q = 1$ (not shown here), we found that the performance is more sensitive to the choice of η than it is the case when $Q = 2$.

Fig. 6(a) and (b) show the performance of the proposed FS, TS, and MF methods as a function of the L_k, the number of paths for each user, when $K = 2, \mathrm{SNR} = 20$ dB, $\mathrm{NFR} = 10$ dB, $f_D T_s = 0.01$, and $M = 150$. We see that for this particular example, as the number of paths increases, all estimators suffer a degradation, although the proposed FS schemes are the best for all L_k. Note, however, that the effect of multipath on code acquisition may be more complicated than that. It has been found in [30]–[32] that on one hand, the weaker paths may lower the overall acquisition probability; on the other, code acquisition may also benefit from the existence of several signal paths, which reduces the mean acquisition time. The impact of multipath on code acquisition may also be complicated by factors such as the number of users in the system, the power of the interfering users, the channel fading rate, and the technique used for acquisition.

Finally, we examine the impact of inaccurate knowledge of the path number on the performance of the proposed estimators. The experimental setup is similar to that of Fig. 4, except that we only consider the case with $\gamma = 2$ for the proposed schemes. Fig. 7(a) and (b) depict the results when L_k, the path number for

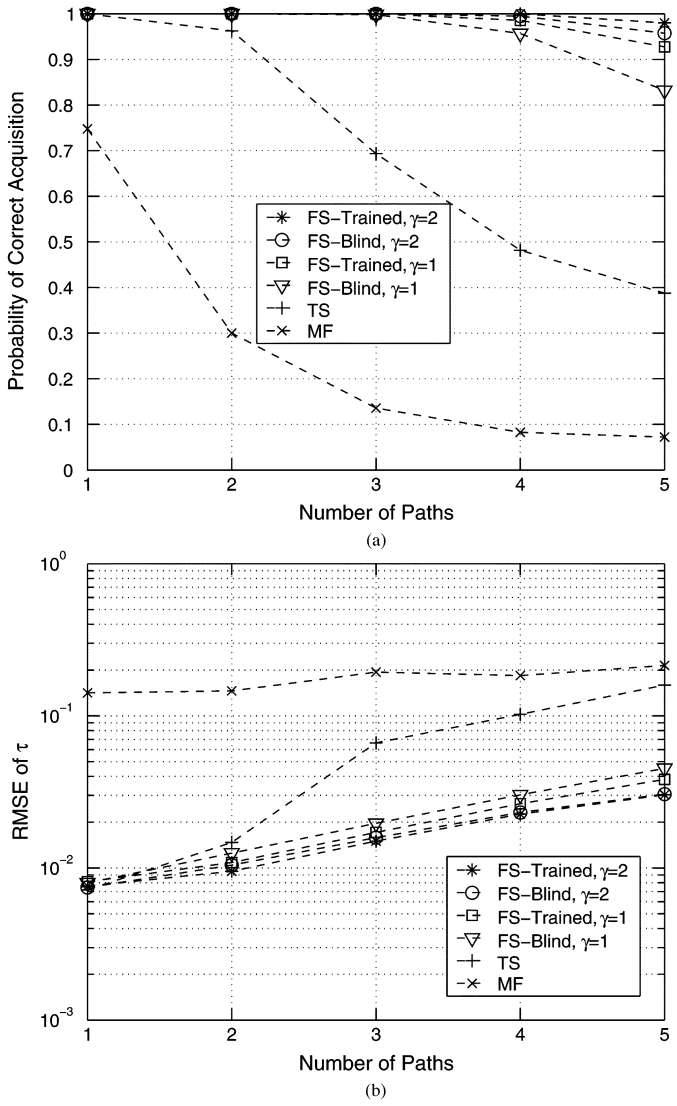

Fig. 6. Performance versus the number of paths in time-varying frequency-selective fading channels when $Q = 2, K = 2, \mathrm{NFR} = 10$ dB, $\mathrm{SNR} = 20$ dB, $M = 150$, and $f_D T_s = 0.01, \forall k$. (a) Probability of correct acquisition. (b) rmse.

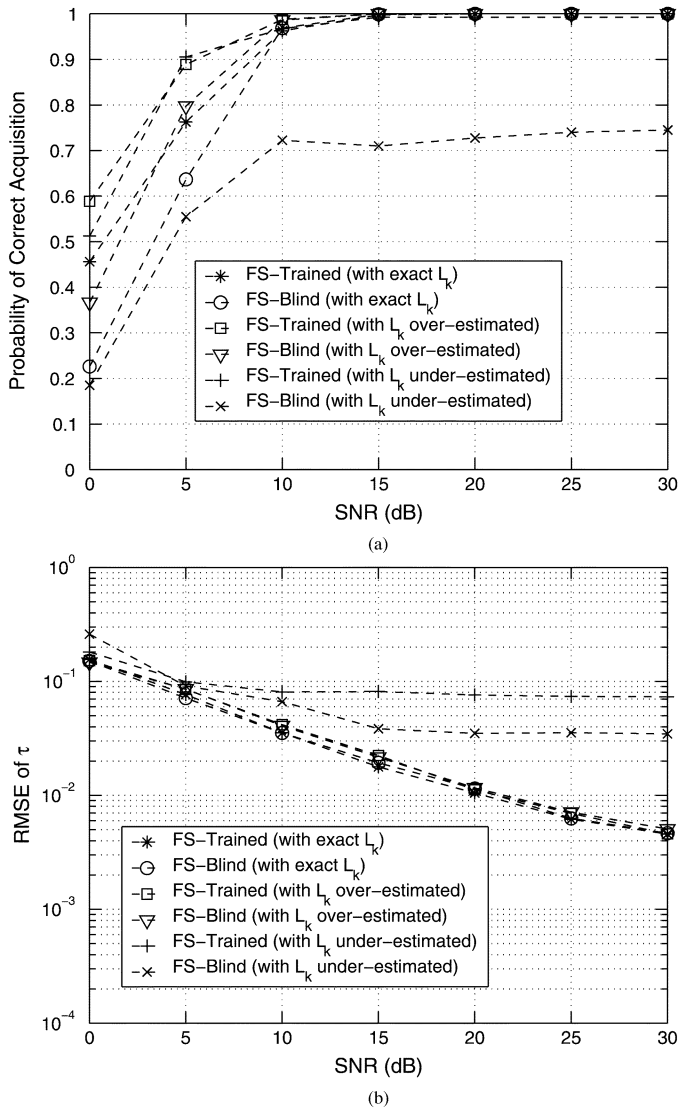

Fig. 7. Performance versus SNR in time-varying frequency-selective fading channels when the number of paths is over- or under-estimated, $\gamma = 2, Q = 2, M = 150, K = 6, \mathrm{NFR} = 10$ dB, $f_D T_s = 0.01$, and $L_k = 2, \forall k$. (a) Probability of correct acquisition. (b) rmse.

the desired user, is known exactly, underestimated by one, and overestimated by one, respectively. It is seen that path overestimation appears to cause little performance loss, while underestimation degrades the proposed schemes considerably. This is because when L_k is underestimated, some signal eigenvectors are mistaken as noise eigenvectors and used for parameter estimation, which degrades the performance since (40) no longer holds. On the other hand, no such mistakes occur with path overestimation. This suggests that we may over-estimate the path number if exact knowledge is not available. However, it should be noted that path over-estimation has the drawback that it produces extra code-timing estimates for paths that do not exist.

VI. Conclusion

We have presented a group of blind and training-assisted code-timing estimation algorithms for CDMA systems with bandlimited chip waveforms. The proposed schemes rely on subspace structure of the received signal in the frequency domain. They can be implemented efficiently through polynomial rooting, and offer the remarkable flexibility to trade off performance, user capacity, and implementation complexity. The proposed schemes are near-far resistant, and able to deal with time- and frequency-selective channel fading. Numerical results show that the proposed frequency-domain based methods outperform an earlier time-domain subspace scheme which requires iterative nonlinear searches, and is plagued by inaccurate parameter initialization.

References

[1] R. Prasad and T. Ojanperä, "An overview of CDMA evolution toward wideband CDMA," *IEEE Commun. Surveys*, vol. 1, no. 1, pp. 2–29, 1998. Fourth Quarter.

[2] R. L. Peterson, R. E. Ziemer, and D. E. Borth, *Introduction to Spread Spectrum Communications*. Englewood Cliffs, NJ: Prentice-Hall, 1995.

[3] S. Verdú, *Multiuser Detection*: Cambridge Press, 1998.

[4] R. F. Smith and S. L. Miller, "Acquisition performance of an adaptive receiver for DS-CDMA," *IEEE Trans. Commun.*, vol. 47, pp. 1416–1424, Sept. 1999.

[5] D. Zheng, J. Li, S. L. Miller, and E. G. Ström, "An efficient code-timing estimator for DS-CDMA system," *IEEE Trans. Signal Processing*, vol. 45, pp. 82–89, Jan. 1997.
[6] Z.-S. Liu, J. Li, and S. L. Miller, "An efficient code-timing estimator for receiver diversity DS-CDMA systems," *IEEE Trans. Commun.*, vol. 46, pp. 826–835, June 1998.
[7] E. G. Ström, S. Parkvall, S. L. Miller, and B. E. Ottersten, "Propagation delay estimation in asynchronous direct-sequence code-division multiple access systems," *IEEE Trans. Commun.*, vol. 44, pp. 84–93, Jan. 1996.
[8] S. E. Bensley and B. Aazhang, "Subspace-based channel estimation for code division multiple access communications systems," *IEEE Trans. Commun.*, vol. 44, pp. 1009–1020, Aug. 1996.
[9] E. G. Ström, S. Parkvall, S. L. Miller, and B. E. Ottersten, "DS-CDMA synchronization in time-varying fading channels," *IEEE J. Select. Areas Commun.*, vol. 14, pp. 1636–1642, Oct. 1996.
[10] T. Östman, S. Parkvall, and B. Ottersten, "An improved MUSIC algorithm for estimation of time delays in asynchronous DS-CDMA systems," *IEEE Trans. Commun.*, vol. 47, pp. 1628–1631, Nov. 1999.
[11] K. Amleh and H. Li, "An algebraic approach to blind carrier offset and code timing estimation for DS-CDMA systems," *IEEE Signal Processing Lett.*, vol. 10, pp. 32–34, Feb. 2003.
[12] U. Madhow, "Blind adaptive interference suppression for the near-far resistant acquisition and demodulation of direct-sequence CDMA signals," *IEEE Trans. Signal Processing*, vol. 45, pp. 124–136, Jan. 1997.
[13] M. Latva-aho, J. Lilleberg, J. Iinatti, and M. Juntti, "CDMA downlink code acquisition performance in frequency-selective fading channels," in *Proc. IEEE Int. Symp. Personal, Indoor, and Mobile Radio Communication (PIMRC'98)*, Boston, MA, Sept. 1998, pp. 1476–1479.
[14] H. Li and R. Wang, "Filterbank-based blind code synchronization for DS-CDMA systems in multipath fading channels," *IEEE Trans. Signal Processing*, vol. 51, pp. 160–161, Jan. 2003.
[15] J. G. Proakis, *Digital Communications*, 3rd ed: McGraw-Hill, 1995.
[16] T. Östman and B. Ottersten, "Near far robust time delay estimation for asynchronous DS-CDMA systems with bandlimited pulse shapes," in *Proc. IEEE 48th Veh. Technol. Conf.*, Ottawa, Canada, May 1998, pp. 1650–1654.
[17] N. Petrochilos and A. J. van der Veen, "Blind time delay estimation in asynchronous CDMA via subspace intersection and ESPRIT," in *Proc. 2001 IEEE Int. Conf. Acoust., Speech, and Signal Processing (ICASSP'2001)*, Salt Lake City, UT, May 2001.
[18] R. Roy and T. Kailath, "ESPRIT-estimation of signal parameters via rotational invariance techniques," *IEEE Trans. Acoust., Speech, Signal Processing*, vol. 37, pp. 984–995, July 1989.
[19] J. G. Proakis, *Digital Communications*, 4th ed. New York: McGraw-Hill, 2000.
[20] W. C. Jakes Jr., *Microwave Mobile Communications*. New York: Wiley-Intersci., 1974.
[21] M. Wax and T. Kailath, "Detection of signals by information theoretic criteria," *IEEE Trans. Acoust., Speech Signal Processing*, vol. 33, pp. 387–392, Apr. 1985.
[22] T. S. Rappaport, *Wireless Communications: Principles and Practice*. Upper Saddle River, NJ: Prentice-Hall, 1996.
[23] A. J. van der Veen, M. C. Vanderveen, and A. Paulraj, "Joint angle and delay estimation using shift-invariance techniques," *IEEE Trans. Signal Processing*, vol. 46, pp. 405–418, Feb. 1998.
[24] A. V. Oppenheim and R. W. Schafer, *Discrete-Time Signal Processing*. Englewood Cliffs, NJ: Prentice Hall, 1989.
[25] P. Stoica and R. L. Moses, *Introduction to Spectral Analysis*. Upper Saddle River, NJ: Prentice-Hall, 1997.
[26] P. Kravanja and M. van Barel, *Computing the Zeros of Analytic Functions*, Berlin: Springer-Verlag, 2000.
[27] J. M. McNamee, A Bibliography on Roots of Polynomials.
[28] T. Söderström and P. Stoica, *System Identification*, London, U.K.: Prentice-Hall Int., 1989.
[29] H. Li, R. Wang, and K. Amleh, "Unconditional CRB for code synchronization in CDMA systems with bandlimited chip waveforms," in *Proc. 36th Annual Conf. Information Sciences and Systems (CISS'02)*. Princeton, NJ, Mar. 2002.
[30] G. Giunta, A. Neri, and M. Carli, "Constrained optimization of noncoherent serial acquisition of spread-spectrum code by exploiting the generalized Q-functions," *IEEE Trans. Veh. Technol.*, vol. 52, pp. 1378–1385, Sept. 2003.
[31] J. H. J. Iinatti, "On the threshold setting principles in code acquisition of DS-SS signals," *IEEE J. Select. Areas Commun.*, vol. 18, pp. 62–72, Jan. 2000.
[32] S. Glisic and M. D. Katz, "Modeling of the code acquisition process for rake receiver in CDMA wireless networks with multipath and transmitter diversity," *IEEE J. Select. Areas Commun.*, vol. 19, pp. 21–32, Jan. 2001.

Khaled Amleh (M'03) received the M.Sc. degree in applied computer mathematics from Long Island University in 1994, the M.Sc. degree in electrical engineering from the New York Institute of Technology in 1996, and the Ph.D. degree in electrical engineering from Stevens Institute of Technology, Hoboken, NJ, in 2003.

From 1999 to 2003, he was an associate instructor with the Department of Electrical and Computer Engineering, Stevens Institute, where he received the Best Instructor Award. His research interest is in the area of wireless communications, with emphasis on signal processing for communications, code division multiple access (CDMA), orthogonal frequency division multiplexing (OFDM), detection and estimation, and stochastic signal processing. He is now an Assistant Professor of Electrical Engineering with Pennsylvania State University, Mont Alto.

Hongbin Li (M'99) received the B.S. and M.S. degrees from the University of Electronic Science and Technology of China (UESTC), Chengdu, in 1991 and 1994, respectively, and the Ph.D. degree from the University of Florida, Gainesville, in 1999, all in electrical engineering.

From July 1996 to May 1999, he was a Research Assistant with the Department of Electrical and Computer Engineering, University of Florida. He was a Summer Visiting Faculty Member with the Air Force Research Laboratory, Rome, NY, during the summers of 2003 and 2004. Since July 1999, he has been an Assistant Professor with the Department of Electrical and Computer Engineering, Stevens Institute of Technology, Hoboken, NJ. His current research interests include wireless communications, statistical signal processing, and radars.

Dr. Li is a member of Tau Beta Pi and Phi Kappa Phi. He received the Harvey N. Davis Teaching Award in 2003 and the Jess H. Davis Memorial Award for excellence in research in 2001 from Stevens Institute of Technology in 2001, and the Sigma Xi Graduate Research Award from the University of Florida in 1999. He is an Editor for the IEEE TRANSACTIONS ON WIRELESS COMMUNICATIONS.

Tao Li received the B.S. and M.S. degrees in computer science in 1986 and 1991, respectively, and the Ph.D. degree in circuits and systems in 1995, all from the University of Electronic Science and Technology of China (UESTC), Chengdu.

From 1993 to 1994 he was a visiting scholar with the University of California, Berkeley. He is currently a Professor with the Department of Computer Science, Sichuan University, China, where he directs the Laboratory of Computer Networks and Information Security. His research interests include computer networks, information security, artificial immune system, neural networks, artificial intelligence, and wireless communications.